Supplementary Information: Inflammation in children with chronic kidney disease linked to gut dysbiosis and metabolite imbalance

Table of content

Supplemental Figures

Figure S1: Study description

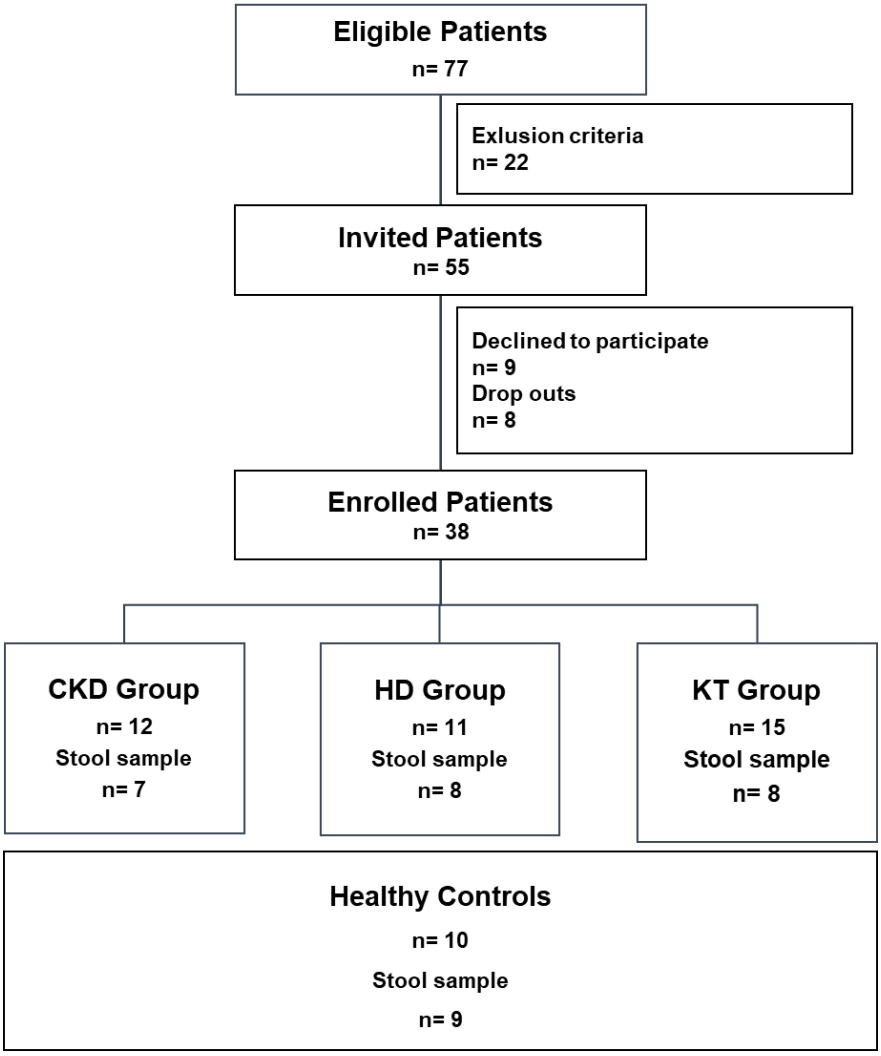

From 77 patients eligible for this study, 55 patients were invited to participate (22 were excluded as they met exclusion criteria). 9 patients or their parents declined to participate and 8 patients were excluded during the recruitment for other reasons (antibiotic treatment, lost to follow-up, difficulty in blood drawing). Moreover, 10 healthy individuals with normal kidney function, treated at the hospital for reasons other than kidney disease, were enrolled to this study.

Abbreviations: CKD = chronic kidney disease; HD = hemodialysis; KT = kidney transplantation.

Figure S2: Microbiome analysis on phylogenetic phylum level

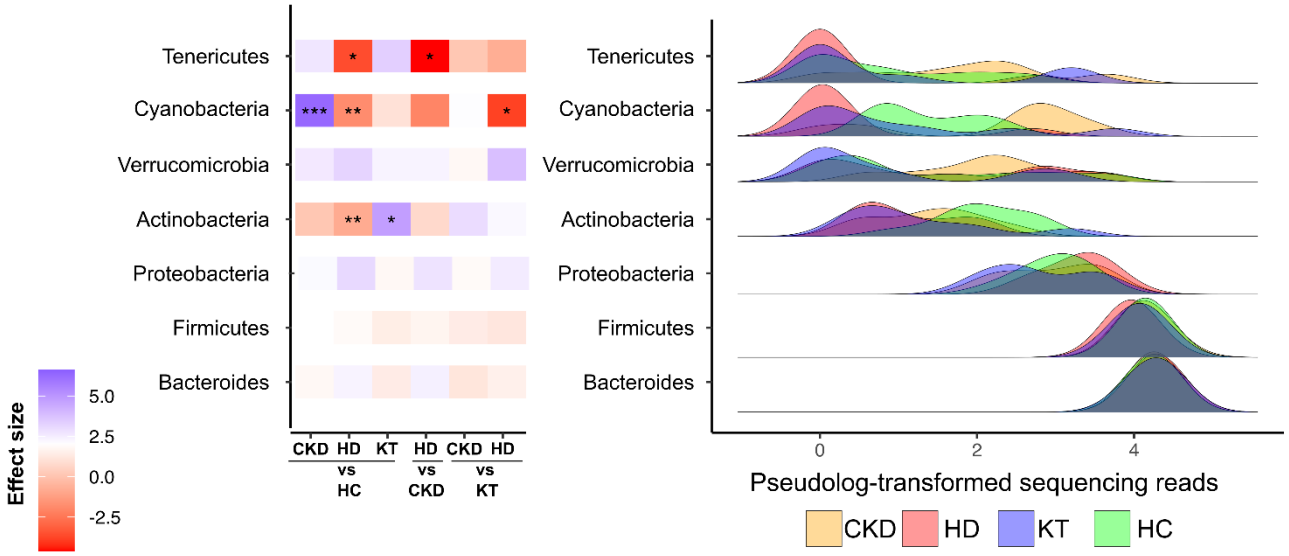

Analysis of gut microbiota from 16S rRNA sequencing in children (n = 32) with chronic kidney disease (CKD G3-4), patients with hemodialysis (HD), patients after kidney transplantation (KT) and healthy controls (HC). Analyses of group differences on phylum level are shown as a heatmap. Patient groups were tested against each other (pairwise). The heatmap shows significant changes in abundance using DESeq2 v1.30.1 package. All significance estimates were adjusted for multiple tests using Benjamini-Hochberg FDR correction. In addition, phylum level abundance is visualized as density plots, stratified by disease status. x-axis shows log10 (relative abundance) of each phylum, y-axis the phylum annotation provided by LotuS.

Figure S3: Phylogenetic tree analysis of 16S amplicon sequencing

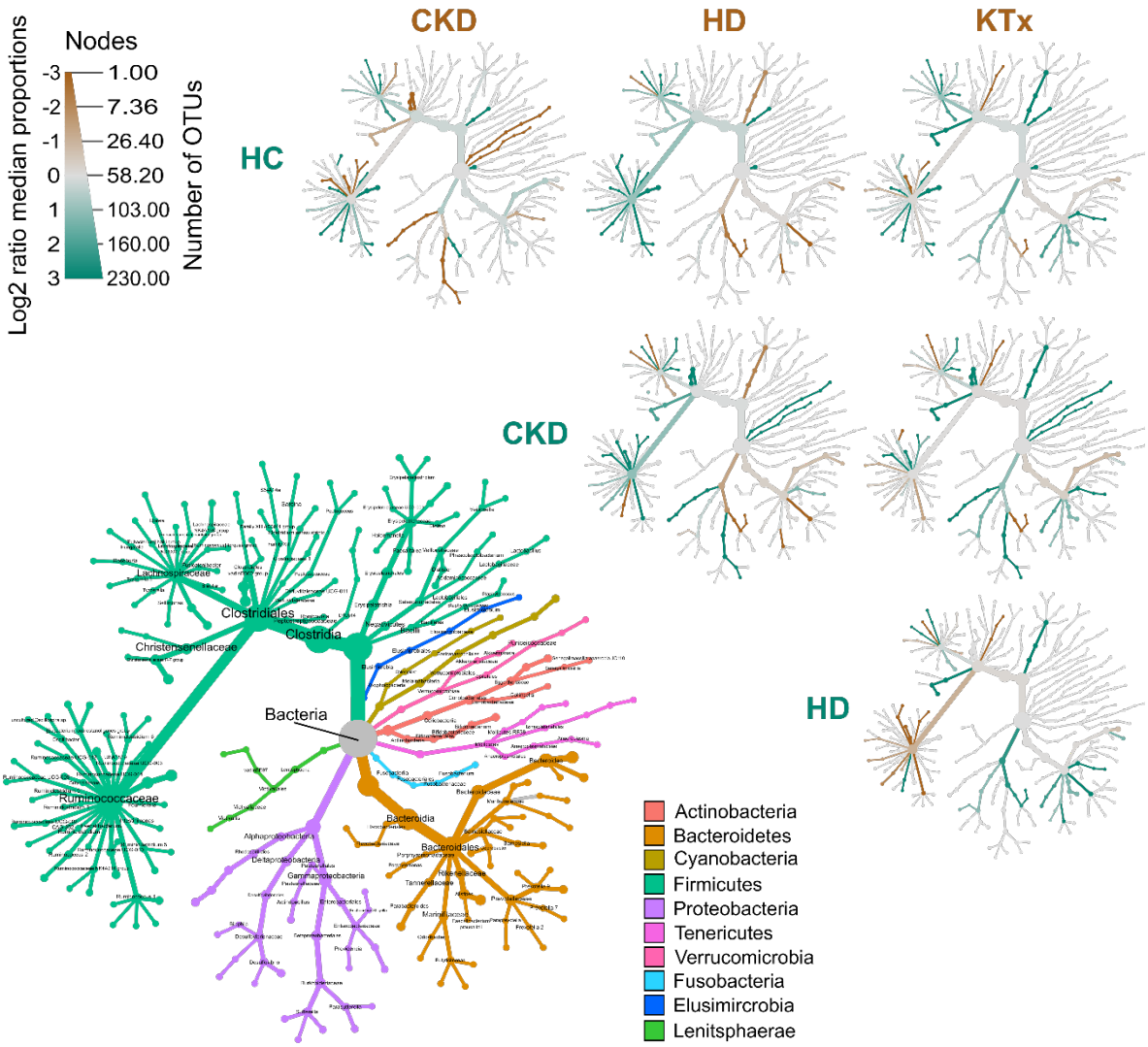

Phylogenetic analysis from 16S rRNA sequencing in children (n = 32) with chronic kidney disease (CKD G3-4), patients with hemodialysis (HD), patients after kidney transplantation (KT) and healthy controls (HC). Phylogenetic tree was constructed using the metacoder R package. Differences between groups are shown as log2 median ratio. Top right panels show group to group comparisons, bottom right tree indicates taxonomic annotations, node size indicates number of OTU per node. Not annotated nodes were not labeled.

Figure S4: Activity of the aryl hydrocarbon receptor in response to different concentrations of indoxyl sulfate

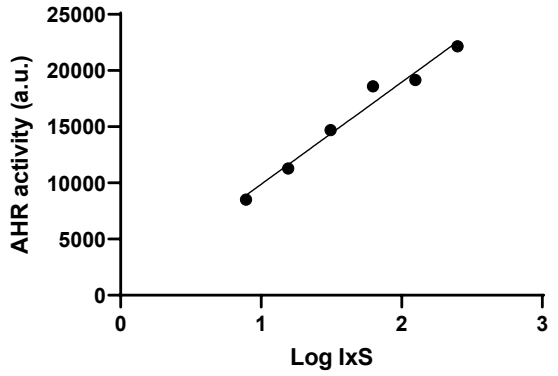

Transfected HT29 reporter cells were incubated with different concentrations of indoxyl sulfate (IxS) for 24 hours. Subsequently, the luciferase activity was measured indicating the activity of the aryl hydrocarbon receptor (AhR).

Figure S5: **Potential for short chain fatty acid (SCFA) production and its serum levels in children with chronic kidney disease**

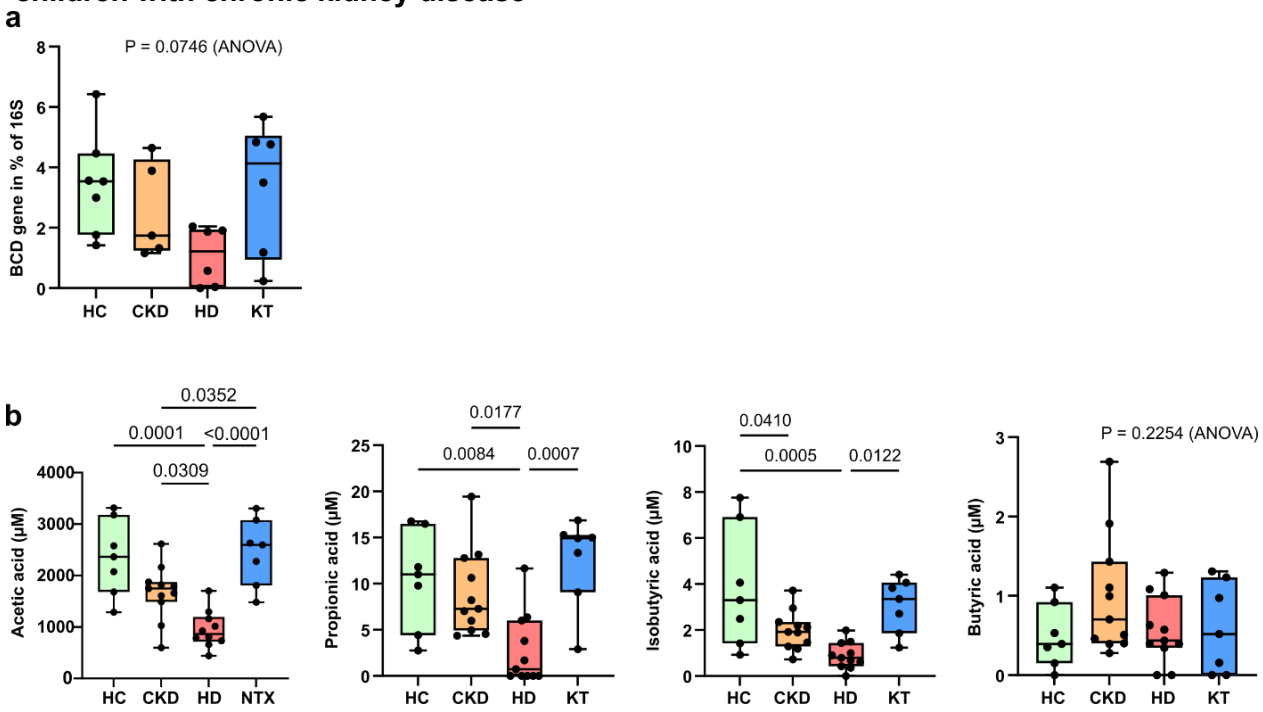

The abundance of the butyrate associated gene Butyryl-CoA-Dehydrogenase (BCD) was analyzed in fecal samples (n=24) showing a lower abundance in patients of the HD group (a). Systemic levels of the SCFA acetate, propionate, isobutyrate and butyrate were analyzed in serum samples (n=36, b). *P* values ≤ 0.05 are shown, as measured by ordinary one-way ANOVA or Kruskal-Wallis test and adjusted by post-hoc Tukey´s or Dunn´s correction for multiple testing. Data is shown as a box (median and interquartile range) and whiskers (min-max) with overlaid dot plot.

Abbreviations: CKD= chronic kidney disease, HD= hemodialysis, KT= kidney transplantation, HC= healthy controls

Figure S6: Systemic levels of TMAO in pediatric CKD

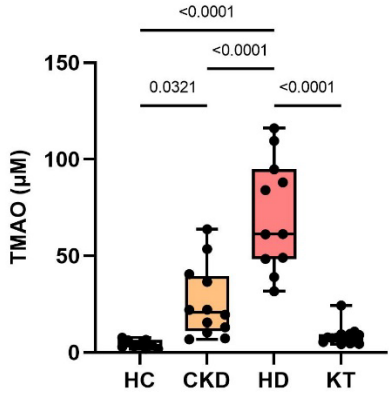

Trimethylamone-N-oxide (TMAO) was measured in plasma samples (n=46) of children at different stages of chronic kidney disease (CKD G3-4), hemodialysis (HD) and patients after kidney transplantation (KT) compared to healthy controls (HC). P values ≤ 0.05 are shown, as measured by ordinary one-way ANOVA and adjusted by post-hoc Tukey´s correction for multiple testing. Data is shown as a box (median and interquartile range) and whiskers (min-max) with overlaid dot plot.

Figure S7: Gating strategy

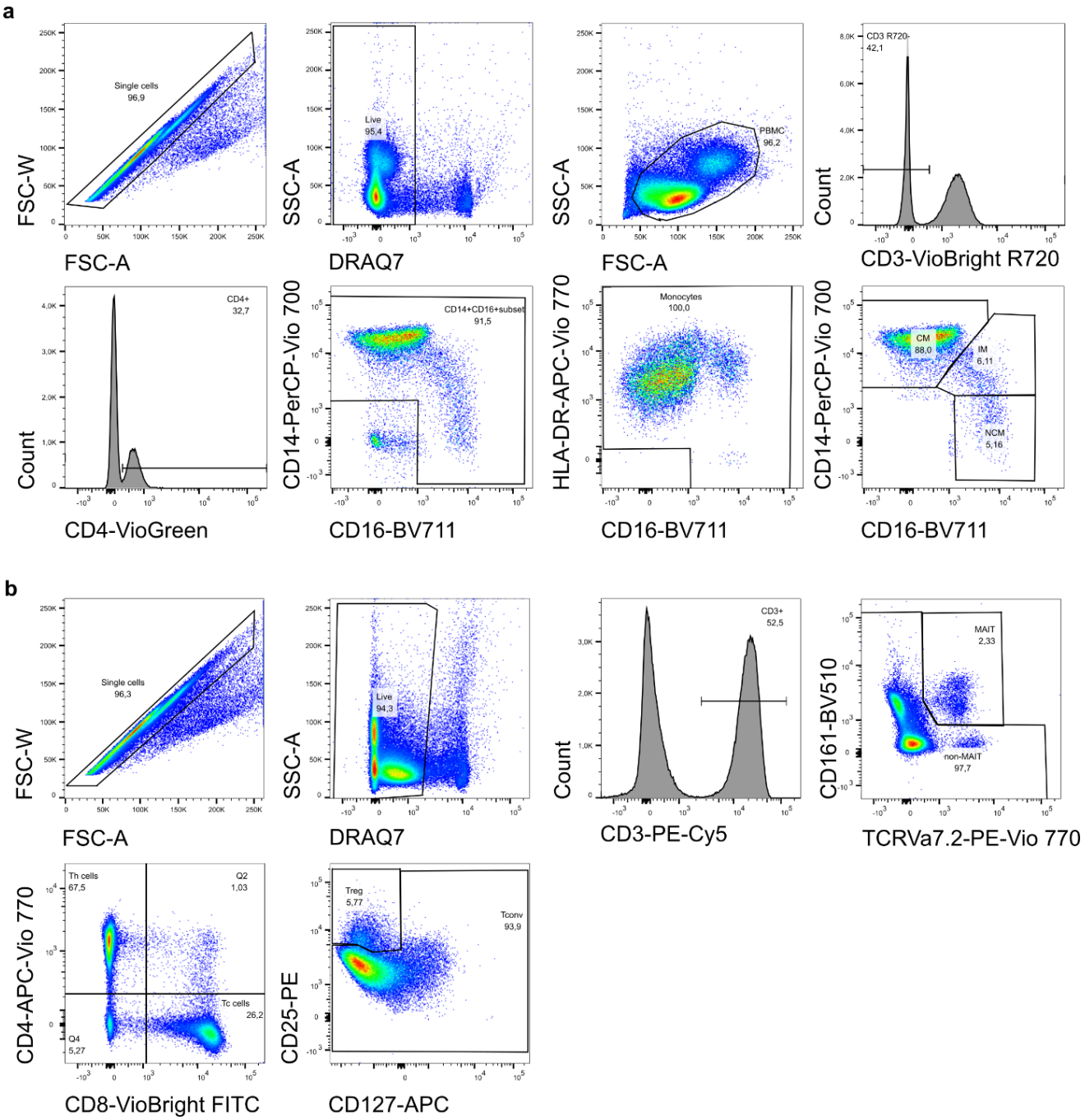

Gating strategy for the analysis of human peripheral blood mononuclear cells for flow cytometry. a) Gating for monocyte subsets. b) Gating for MAIT cells and Treg.

Abbreviations: PBMC= peripheral blood mononucleated cells; MAIT cells= mucosa associated invariant t cells; Treg= regulatory T cells; CM= classical monocytes; IM= intermediate monocytes; NCM= non-classical monocytes; Th= T helper; Tc= T cytotoxic; Tcon= T conventional.

Figure S8: Dendritic cell differentiation in human peripheral blood mononuclear cells

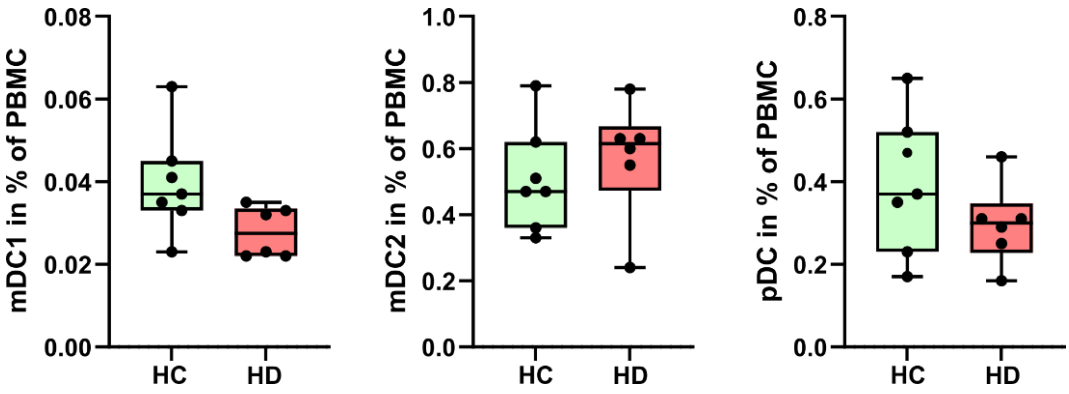

The relative abundance (in % of peripheral blood mononuclear cells (PBMC)) is shown for myeloid dendritic cells type 1 (mDC1: HLA-DR+CD141+CleC9a+), mDC2 (HLA-DR+, CD1c+, CD11c+) and plasmacytoid DC (pDC: HLA-DR+, CD123+) in HD (n=6) and HC (n=7) individuals. *P* values ≤ 0.05 are shown as analyzed by t test or Mann-Whitney-U test.

Figure S9: Hierarchical gating of mucosa-associated invariant T cells and regulatory T cells

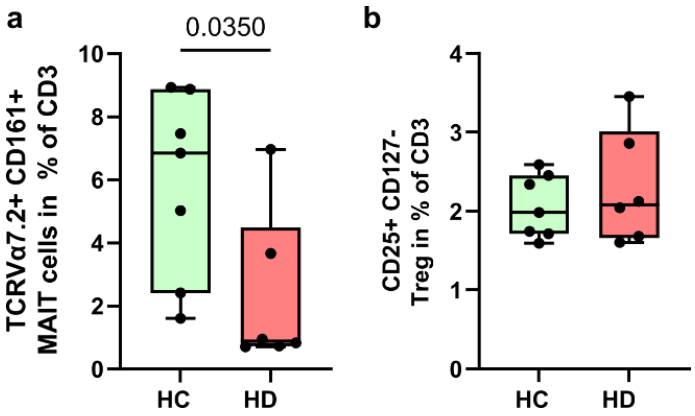

The relative abundance (in % of CD3+ T cells) is shown for mucosa-associated invariant T (MAIT) cells, defined as CD161+TCRVa7.2+ (a) and regulatory T cells (Treg), defined as CD25+CD127- in HD (n=6) and HC (n=7) individuals. *P* values ≤ 0.05 are shown as analyzed by t test or Mann-Whitney-U test.

Supplemental Tables

Table S1: Antibodies used for flow cytometry

Antibodies (Monocytes/DC)	Dilution	Source	Identifier
CD123, FITC, clone REA918	1:50	Miltenyi	#130-115-269
CD14, PerCP-Vio 700, clone REA599	1:400	Miltenyi	#130-110-523
CleC9a, APC, clone REA976	1:50	Miltenyi	#130-116-354
HLA-DR, APC-Vio 770, clone REA805	1:50	Miltenyi	#130-111-792
CD3, VioBright R720, clone REA613	1:50	Miltenyi	#130-127-377
CD8, BV786, clone RPA-T8	1:20	BL	#301046
CD16, BV711, clone 3G8	1:20	BL	#302044
CD11c, BV650, clone Bu15	1:20	BL	#337283
CD141, BV605, clone M80	1:20	BL	#344118
CD4, VioGreen, clone VIT4	1:50	Miltenyi	#130-113-221
CD142, BV421, clone HTF-1	1:10	Miltenyi	#130-098-921
CD163, PE-Vio 770, clone REA179	1:50	Miltenyi	#130-112-130
DRAQ7 (L/D)	1:500	Miltenyi	#130-117-342
CD1c, PE-Vio 615, clone REA694	1:50	Miltenyi	#130-114-547
CD42b, PE, clone REA185	1:50	Miltenyi	#130-123-725
Antibodies (T surface)	**Dilution**	**Source**	**Identifier**
CD8, VioBright FITC, clone BW135/80	1:50	Miltenyi	#130-113-163
CCR10, PerCP-Vio 700, clone 1B5	1:25	BD	#564772
CD127, APC, clone REA614	1:50	Miltenyi	#130-113-413
CD4, APC-Vio 770, clone REA623	1:50	Miltenyi	#130-113-223
CD45RA, BV786, clone HI100	1:50	BD	#563870
CXCR3, BV711, clone GO25H7	1:20	BL	#353732
CD27, BV650, clone L128	1:25	BD	#563228
CCR6, BV605, clone GO34E3	1:20	BL	#353420
CD161, BV510, clone HP-3G10	1:20	BL	#339922
CCR8, BV421, clone 433-H	1:20	BD	#566379
TCRVa7.2, PE-Vio770, clone REA179	1:10	Miltenyi	#130-100-206
DRAQ7 (L/D)	1:500	Miltenyi	#130-117-342
CD3, PE-Cy5, clone UCHT1	1:20	BD	#555334
CCR4, PE-CF594, clone L291H4	1:20	BL	#359420
CD25, PE, clone REA945	1:50	Miltenyi	#130-115-534

Antibodies (T activation)	Dilution	Source	Identifier
PD-1 VioBright B515, clone REA1165	1:50	Miltenyi	#130-120-386
CD8, PerCP-Vio 700, clone BW135/80	1:50	Miltenyi	#130-113-161
CD69, APC, clone REA824	1:50	Miltenyi	#130-112-614
CD3, APC-Vio 770, clone REA613	1:50	Miltenyi	#130-113-136
BD Viability Stain 700	1:1000	BD	#564997
CD45RA, BV786, clone HI100	1:25	BD	#563870
CD31, BV711, clone WM59	1:25	BL	#303136
CD161, BV650, clone DX12	1:20	BD	#563864
CD39, BV605, clone A1	1:25	BL	#328236
CD25, BV510, clone M-A251	1:20	BD	#563352
TCRVa7.2, VioBlue, clone REA179	1:10	Miltenyi	#130-100-209
CD127, PE-Vio 770, clone REA614	1:50	Miltenyi	#130-113-415
CD4, PE-Cy5, clone RPA-T4	1:25	BD	#555348
CD62L, PE-CF594, clone DREG-56	1:25	BD	#562301
FoxP3, PE, clone 259D	1:20	BL	#320108
Antibodies (MAIT cytokines)	**Dilution**	**Source**	**Identifier**
TCRVa7.2 FITC, clone REA179	1:50	Miltenyi	#130-123-685
IL22, APC, clone REA466	1:10	Miltenyi	#130-111-768
IL17A, APC-Vio 770, clone CZ8-23G1	1:50	Miltenyi	#130-120-409
TNFa, R718, clone Mab11	1:20	BD	#566957
CD3, BV786, clone SK7	1:100	BD	#563870
IFNg, BV711, clone B27	1:20	BD	#564039
CD8, BV650, clone SK1	1:100	BL	#344730
IL2, BV605, clone 5344,111	1:20	BD	#563947
Ki-67, BV510, clone B56	1:20	BD	#563462
GRZB, BV421, clone GB11	1:400	BD	#563389
CD161, PE-Vio 770, clone REA631	1:50	Miltenyi	#130-113-597
CD4, PE-Cy5, clone RPA-T4	1:20	BD	#555348
BD Viabilty Stain 620	1:500	BD	#564996
GMCSF, PE, clone REA1215	1:50	Miltenyi	#113-123-419

Table S2: **Markers of inflammation in children with CKD and healthy individuals at study enrolment**

	HC	CKD G3-4	HD	KT
Patients (n)	9	12	11	14
TNF-a	2.87 ± 1.10	7.54 ± 2.22	9.63 ± 2.73	5.70 ± 1.66
Interleukin 2	0.40 ±0.17	0.53 ± 0.68	0.34 ± 0.0	0.42 ± 0.32
Interleukin 4	0.06 ± 0.01	0.05 ± 0.002	0.06 ± 0.01	0.05 ± 0
Interleukin 6	0.73 ± 0.65	1.06 ± 0.84	1.39 ± 1.03	1.05 ± 0.94
Interleukin 8	5.39 ± 1.85	6.52 ± 3.18	7.21 ± 3.58	10.63 ± 10.81
Interleukin 10	0.60 ± 0.48	0.54 ± 0.49	0.44 ± 0.33	0.72 ± 0.76
Interleukin 13	0.30 ± 0.34	0.19 ± 0.15	0.18 ± 0.10	0.35 ± 0.40
Interleukin 1-β	0.59 ± 1.35	0.19 ± 0.18	1.00 ± 2.13	0.16 ± 0.08
Interleukin 12p70	0.18 ± 0.07	0.22 ± 0.15	0.19 ± 0.11	0.21 ± 0.16
Interferon y	6.37 ± 10.2	1.06 ± 0.84	1.27 ± 1.06	5.05 ± 7.28

Cytokines were measured in 46 patients at time of study enrolment. Patients were grouped into four categories (CKD= chronic kidney disease, HD= hemodialysis, KT= kidney transplantation, HC= healthy controls). Data is shown as mean ± standard deviation.

Table S3: **Multivariable ANOVAs on possible confounders influencing the serum levels of tryptophan metabolites in children with chronic kidney disease**

Metabolite	Age (years)	BMI (kg/m^2)	Disease	eGFR ($ml/min/1.73m^2$)	Group	Ethnic Bachground	Gender
3OH-Kynurenin	0.56	1	1	0.23	<0.001	0.23	1
5OH-Tryptophan	1	1	1	0.02	0.72	1	0.44
Anthranilic acid	1	1	1	1	<0.001	1	1
Indole-3-carboxyaldehyde	1	1	1	0.99	1	1	1
Indole-3-propionate	1	1	1	1	1	1	1
Indole lactate	1	1	1	0.06	<0.001	1	1
Indoxyl sulfate	1	1	1	1	<0.001	1	1
Kynurenin/Tryptophan	1	1	1	1	<0.001	1	1
Kynurenic acid	1	1	1	1	<0.001	1	1
Kynurenine	1	1	1	1	0.001	1	1
Tryptamin	1	1	1	1	1	1	1
Tryptophan	1	1	1	1	<0.001	1	1
Xanthurenic acid	1	1	1	1	0.001	0.61	1

Multivariable ANOVAs revealed a significant influence of patient group (CKD, HD, KT, HC) on the plasma levels of tryptophan metabolites in 48 children with CKD. Age, BMI, underlying kidney disease, eGFR, ethnic background and gender had no influence on plasma metabolite levels. All significance estimates were adjusted for multiple tests using Benjamini-Hochberg FDR correction.

Abbreviations: BMI= body mass index, eGFR= estimated glomerular filtration rate, CKD= chronic kidney disease, HD= hemodialyis, KT= kidney transplantation, HC= healthy controls.

Table S4: **Tryptophan metabolite transitions**

Compound	Acquisition Mode	Precursor Ion *(m/z)*	Qualifier Ion *(m/z)*	Qualifier Ion *(m/z)*	Qualifier Ion *(m/z)*	Qualifier Ion *(m/z)*	Retention Time (min)
3-Hydroxykynurenine	pos	225.2100	207.8200	162.3800	110.2000		2,2
5-Hydroxytryptophan	pos	221.0920	204.0660	162.0550			2.5
6-Hydroxymelatonin	pos	249.1230	190.0400	158.0000			3.4
Anthranilate	pos	138.0540	120.0450	92.0140	65.0390		3.3
Indole-3-carboxaldehyde	pos	146.0600	91.0400	117.0400	89.0400	65.1000	4.0
Indole-3-propionic acid	pos	190.0860	130.0580	128.0400	103.0580		4.1
Indolelactate	pos	206.0810	118.0650	130.0650			3.6
Indoxylsulfate Kynurenic	neg	212.0020	132.3700	80.1600			2.8
acid Kynurenine	pos	190.0940	144.0500	116.3750	89.2000		3.4
Melatonin	pos	209.0920	94.0400	118.0790			2.5
Serotonin	pos	233.1280	174.0000	159.0000			3.9
Tryptamine Tryptophan	pos	177.1020	160.0760	132.0450	115.0330		2.5
Xanthurenic acid	pos	161.1070	117.0700	144.0810			2.9
	pos	205.0970	118.2000	115.0400			3.0
	pos	206.0440	160.0400	187.9290	178.0000	132.0450	3.3

Supplemental Methods

Clinical assessment, biobanking and routine laboratory measurements

At the time of enrolment, we obtained baseline demographic (age, gender, diagnosis, ethnic background, body weight and height) and clinical data from all patients. eGFR was calculated according to the bedside formula of Schwartz based on serum creatinine[1], percentiles of weight and BMI were determined according to national references[2]. Office systolic and diastolic blood pressures were documented as an average of three oscillometric measurements using local devices and normalized to national references[3]. Arterial hypertension was defined as blood pressure values above the 95th percentile.

Heparinized blood specimens were collected as part of routine laboratory sampling and used for the measurement of creatinine, urea, uric acid, phosphate, albumin, C-reactive protein (CrP), parathyroid hormone (PTH), and triglyceride levels. Serum, EDTA and Heparin plasma were stored at -80°C until further use. For the measurement of TNF-α, IL-2, IL-4, IL-6, IL-8, IL-1β, IL-10, IL-13, IL-12p70, and IFN-y, plasma was analyzed using the Meso Scale Discovery (MSD) V-PLEX Plus Proinflammatory Panel 1 (human) according to the manufacturer's protocol. All samples were run on a single plate on an MSD plate reader (model 1250). Zonulin-1 (Zo-1) and soluble CD14 (sCD14) were analyzed in patients serum using the human Zo-1 ELISA kit (Biomatik Corporation, Canada) and sCD14 Quantikine ELISA kit (R&D Systems, USA) according to manufacturer's protocol.

Peripheral blood mononuclear cells (PBMC) were isolated by density gradation using Pancoll (Pan Biotech, Germany) using standard protocols and stored in liquid nitrogen until usage.

Stool specimens (2-4g) were collected (Sarstedt, Germany; #80.623.022) and stored for 24 hours at 4 - 8°C max. and transferred to the study center for freezing at -80°C until further use. Patients and parents were provided with detailed information about collection, storage and transport of stool specimens.

Generation of 16S rRNA Amplicon Libraries and Sequencing

Stool DNA was isolated using QIAamp® Fast DNA Stool Mini Kit (QIAGEN, Hilden, Germany) according to manufacturer's protocol. The extracted DNA was used as a template to amplify the V3-V4 region of the bacterial 16S rRNA gene using fusion primers TCGTCGGCAGCGTCAGATGTGTATAAGAGACAG-CCTACGGGNGGCWGCAG (MiSeq_overhang-D-Bact-0341-b-S-17) and GTCTCGTGGGCTCGGAGATGTGTATAAGAGACAG-GACTACHVGGGTATCTAATCC (MiSeq_overhang-S-D-Bact-0785-a-A-21) including bacteria targeting primers[4]. The PCR reaction mixture with a total volume of 25 µl contained 12,5 µl KAPA HiFi HotStart ReadyMix (Roche), 1,25 µl of each primer (10 nM) and 3 ng/µl of isolated DNA. Thermal cycling scheme for bacterial amplicons was as follows: initial denaturation for 3 min at 95°C, 25 cycles at 95°C for 30 s, 30 s at 55°C, and 30 s at 72°C and a final extension at 72°C for 5 min. For each sample, three independent 16S amplicons were generated. The resulting PCR products were purified with Agencourt AMPure XP magnetic beads (Beckman coulter, Krefeld, Germany) and then quantified with Quant-iT dsDNA HS assay kit and a Qubit fluorometer (Invitrogen GmbH, Karlsruhe, Germany) following the manufacturer´s instructions. The three individual, purified V3-V4 PCR products per sample were pooled and used to attach indices and Illumina sequencing adapters using the Nextera XT Index kit (Illumina, CA, USA). Index PCR was performed using 5 µl of template PCR product (each 2 ng/µl), 2.5 µl of each index primer, 12.5 µl of 2× KAPA HiFi HotStart ReadyMix and 2.5 µl PCR grade water. Thermal cycling scheme was as follows: 95°C for 3 min, 8 cycles of 30 s at 95°C, 30 s at 55°C and 30 s at 72°C, and a final extension at 72°C for 5 min. Bacterial 16S Amplicon libraries were sequenced using the dual index paired-end (v3, 2×300 bp) approach for the Illumina MiSeq platform as recommended by the manufacturer.16S amplicon sequences were filtered, quality controlled and taxonomically assigned using the LotuS pipeline[5] with default parameters using the SILVA database (v138). Resulting abundance tables were normalized using the rarefaction toolkit (RTK) using default settings[6].

Phylogenetic Tree

The data retrieved from the Lotus analysis pipeline were further processed using the R package metacoder (v. 0.3.5.001). OTUs with less than 50 reads were discarded and samples were rarefied using the function calc_obs_props. Differences between groups were calculated using the compare_groups function and the log2 median ratio was used to visualize trending differences in abundance between groups in taxonomic trees.

Real Time PCR

PCRs were carried out using a Quantstudio 3 (Applied Biosciences, CA, USA) thermal cycler in a reaction volume of 20µl Taqman fast universal master mix (Applied Biosciences) with Taqman gene expression assay for the butyrate associated bacterial gene Butyryl-CoA-Dehydrogenase (BCD). 50ng of bacterial genomic DNA was used as template and all qPCR was carried out at 60°C in fast mode and primer and probe concentrations were set to 750nM and 250nM, respectively. Gene abundancy was determined relative to bacterial 16s rRNA gene.

Targeted metabolomics

The analysis of plasma metabolites was focused on tryptophan metabolites and short chain fatty acids (SCFA). For the tryptophan analysis, liquid chromatography – mass spectrometry (LC-MS) analysis was performed with a 1290 Infinity 2D HPLC system (Agilent Technologies, USA) combined with a TSQ Quantiva triple quadrupole mass spectrometer with a heated ESI source (Thermo Scientific, USA). Before starting, an extracting solvent was prepared comprising 90% methanol, 0.15 µg/mL mixed internal standards, 0.02% ascorbic acid, and 0.2% formic acid. This was placed at -20°C to cool. For each sample, 280 µL pre-chilled extracting solvent was added to 150ul of EDTA plasma. Samples were held at 4°C and shaken for 15 min at 2000rpm (Eppendorf ThermoMixer C) before being centrifuged for 15 min at 11000g and 4 °C. The supernatant was transferred to a dark LC-MS vial for LC-MS/MS

analysis. 20µl of each plasma sample was pooled, and the pooled plasma was also extracted to make quality control (QC) samples. These QC samples were run every 6 samples.

LC-MS analysis was combined with a triple quadrupole mass spectrometer using a 10-min gradient. A reversed-phase column was used (VisionHT C18 Basic; L × I.D. 150 mm × 4.6 mm, 3 µm particle size, Dr Maisch, Germany) and held at a constant temperature of 30°C. The mobile phase consisted of 0.2 % formic acid in H_2O (solvent A) and 0.2 % formic acid in methanol (solvent B). The following gradient was run with a constant flow rate of 0.4 ml min^{-1}: A/B 97/3 (0 min), 70/30 (from 1.2 min), 40/60 (from 2.7 to 3.75 min), 5/95 (from 4.5 to 6.6 min) and 97/3 (from 6.75 to 10 min). Before starting, the LC-MS was conditioned by running 10 blank (solvent A) and 3 QC samples for 130 min. The molecular ion and at least two transitions were monitored for the 15 metabolites that are part of the tryptophan pathway. Transitions are shown in Table S4.

Data was exported into Skyline v.19.1 - 64 bit to identify and quantify peak intensity and area. Transition settings in the Skyline search were: isotopic peaks included: count; precursor mass analyzer: QIT; acquisition method: targeted; product mass analyzer: QIT. Method match searching tolerance was 0.6 m/z, and data was manually checked to ensure the correct peaks were selected. Cubic spline drift correction was applied per metabolite and to all sample types using the pooled QC samples as references to fit the splines[7,8]. The first and the last QC samples used to fit the cubic splines are the most critical to the resulting fit. In this case, the last conditioning pooled QC sample and the first of two pooled QC replicates at the end of the analytical run were used as the first and last QC respectively in the batch correction. QCs analyzed before or after these timepoints were disregarded for further analysis. For indole-lactate, both end replicates had to be removed as outliers due to clear deviation in areas, and further processing was limited to samples up to the last valid pooled QC sample. Standard samples of increasing concentration were used to construct calibrations curves using linear fits per metabolite. Concentration values less or equal to zero were declared as missing. In this study, several study groups featured measurements systematically outside of the

calibration range for some metabolites (i.e. below or above the smallest or largest standard sample applied for a metabolites calibration curve, respectively). Further, calibration of QC standard samples resulted in insufficient accuracy. However, precision (%RSD in either standard or pooled QC samples) was adequate for most compounds. Hence, metabolites can not be considered as absolutely but as relatively quantified in this study. Three out of 15 TRP metabolites (tryptophan, 5-OH-tryptophan, tryptamin, kynurenine, 3-OH-kynurenine, kynurenic acid, anthranilic acid, xanthurenic acid, IxS, indole-3-carboxyaldehyde, indole-3-propionic acid, indole lactate, 6-OH-melatonin, melatonin, serotonin) were rejected due to relative standard deviation (RSD) higher than 15%, including 6-OH-melatonin, melatonin and serotonin.

SCFA were analyzed by gas chromatography – mass spectrometry (GC – MS). In brief, 90µl serum were mixed with internal standard (100µM crotonic acid (Sigma Aldrich)), 10µl HCL-37% (Sigma Aldrich) and 100 µL diethylether (Sigma Aldrich). Samples were shaken for 30 min at 1500 rpm at 25°C and then centrifuged for 10 min at 1500×g. 50µl of the upper organic phase were transferred to a Chromacol™ glass vial (Thermo Scientific), containing 10µl N-tert-butyldimethylsilyl-N-methyltrifluoroacetamide (MTBSTFA, Sigma Aldrich). Samples were shaken for 30 min at 80°C at 600rpm and subsequently incubated at RT for 24 hours for derivatization. Serial dilutions of SCFA were processed and analysed in parallel for absolute quantification.

GC-MS analysis was performed on a Trace 1310 GC – Q Exactive MS, coupled to a TriPlus RSH autosampler (Thermo Fisher Scientific). Samples were injected in split mode (injection volume 1µL, split 1:10). The following temperature program was applied during sample injection: initial temperature of 80°C for 3 s followed by a ramp of 7°C/sec to 210°C and final hold for 3 min. Gas chromatographic separation was performed with a TG-5SILMS column (30m length, 250µm inner diameter, 0.25µm film thickness (Thermo Fisher)). Helium was used as carrier gas with a flow rate of 1.2 ml/min. Gas chromatographic separation was performed with the following temperature gradient: 2 min initial hold at 68°C, first temperature gradient

with 7°C/min up to 150°C, and second temperature gradient with 50°C/min up to 300°C, with a final hold for 2 min. The spectra were recorded in a mass range of 65 to 600m/z with a resolution of 60,000.

Data was analyzed with Xcalibur QuantBrowser, using serial dilutions of SCFA (ranging from 500nM to 50µM) as well as internal standard (crotonic acid) calibration for quantification (linear fit of area-ratio (SCFA/InternalStandard) to concentration, with 1/X weighting). Following masses were quantified: 131.0524 m/z for propionate, 145.0680 m/z for iso-butyrate and butyrate, and 143.0523 m/z for crotonic acid.

For the determination of trimethylamine-N-oxide (TMAO) plasma levels by LC-MS/MS frozen plasma samples were thawed at room temperature and subsequently 20µl of each was mixed with 80µl of the internal standard d9-TMAO (1µM in methanol) (CDN Isotopes, Pointe-Claire, Canada). Plasma proteins were precipitated by vortexing for 1min. The supernatant was obtained by centrifugation at 16,000g at 4°C for 10min and subjected to LC-MS/MS TMAO quantification applying the multiple reaction monitoring (MRM) approach. Chromatographic separation was achieved on a 1290 Infinity II HPLC (Agilent Technologies, Waldbronn, Germany) equipped with a Poroshell 120 EC-C18 column (3.0 x 150mm, 2.7µm; Agilent Technologies) guarded by a pre-column (3.0 x 5mm, 2.7µm) of identical material. Water (eluent A) and acetonitrile (eluent B), both acidified with 0.1% formic acid, were pumped with 0.25ml/min. Elution of TMAO and its internal standard was achieved with a 5-min linear gradient from 0% to 10% eluent B. Total run-time was 12min including re-equilibration of the LC system. MS/MS analyses were carried out using an Ultivo triple-quadrupole mass spectrometer (Agilent Technologies) operating in the positive electrospray ionization mode (ESI+). The following ion source parameters were set: sheath gas temperature, 400°C; sheath gas flow, 12l/min of nitrogen; nebulizer pressure, 30psi; drying gas temperature, 100°C; drying gas flow, 10l/min of nitrogen; capillary voltage, 2.5kV; nozzle voltage, 0kV. The following mass transitions were recorded (fragmentor voltage [FV] and collision energies [CE] in parentheses):

TMAO: *m/z* 76.1 → 42.1 (FV: 81V, CE: 40eV), *m/z* 76.1 → 58.0 (FV: 81V, CE: 20eV), *m/z* 76.1 → 59.1 (FV: 81V, CE: 8eV); d_9-TMAO: *m/z* 85.1 → 46.1 (FV: 101V, CE: 48eV), *m/z* 85.1 → 66.1 (FV: 101V, CE: 20eV), *m/z* 85.1 → 68.0 (FV: 101V, CE: 12eV). The loss of H_2O (*m/z* 76.1 → 58.0 for TMAO) and HDO (*m/z* 85.1 → 66.1 for d_9-TMAO) was used for quantification[9]. Peak areas were determined with MassHunter Software (Agilent Technologies) and TMAO was directly quantified via its internal standard d_9-TMAO that was concentrated to 0.8µM in the samples.

Metabolomics data is accessible via Metabolights (www.ebi.ac.uk/metabolights/MTBLS5066)[10].

Aryl hydrocarbon receptor (AhR) activity assay

As a method to detect AhR agonists we used a human cell line stably transfected with a reporter plasmid containing an AhR responsive promoter element (HT-29-AhR (InvivoGen, CA, USA)). The XRE is activated upon ligand binding to the AhR and drives the expression of the detectable reporter lucia luciferase. HT-29-AhR cell line (InvivoGen, CA, USA) was grown and maintained in Dulbecco's Modified Eagle Medium (DMEM, Sigma Aldrich) supplemented with 4.5g/l glucose (Sigma Aldrich), 2mM L-glutamine (Sigma Aldrich), 10% (v/v) heat-inactivated fetal bovine serum (Biochrom, Germany), 100 µg/ml Zeocin (Sigma Aldrich) and 100 ug/ml Penicillin-Streptomycin (Sigma Aldrich). For the AhR reporter assay cells at 80% confluency were harvested and re-suspended at 2.8 x 10^5 cells/ml. 20µl of patient serum was mixed with 180µl of cell suspension in a white 96 well plate (Corning, NY, USA). The plate was incubated at 37°C with 5% CO2 for 48h. After 48h, 20µl of cell supernatant was taken from each well and the lucia luciferase was quantified by incubating with Quanti-luc reagent (InvivoGen) according to manufacturer's instructions. Assays were performed in triplicates and luciferase activity was quantified as relative luminescence units (RLU) using a microplate reader (Infinite 200 plate reader, Tecan, Switzerland). The luminescent signal representing ligand induced AhR activity from sera was normalized to the signal of non-inoculated media.

Monocyte isolation and serum incubation

PBMC were isolated from a healthy donors and monocytes were enriched using CD14 MicroBeads (Milteny Biotec, USA) according to manufacturer´s protocol. On a 96 well plate $1x10^6$ cells were plated and incubated for 24 hours at 37°C in standard culture medium containing 20% patient serum, IxS (IxS potassium salt, Sigma Aldrich, USA) at concentrations of 50µM and 125µM or the synthetic AhR antagonist (CH-223191, Sigma Aldrich, USA) respectively. Afterwards, TNF-α was measured in the supernatant using a human TNF-α ELISA kit (Thermo Fisher, USA) according to manufacturer´s protocol.

Flow cytometry analysis

PBMC were analysed by multi-colour flow cytometry. To avoid batch effects, all collected cells were thawed and measured at the same time. After thawing, cells were either stained immediately in FACS buffer or restimulated in a final volume of 200 µl RPMI 1640 (Sigma-Aldrich, USA)) supplemented with 10% FBS (Merck), 100 U/ml penicillin (Sigma-Aldrich, USA), 100 mg/ml streptomycin (Sigma-Aldrich, USA), 50 ng/ml PMA (Sigma-Aldrich, USA), 250 ng/ml ionomycin (Sigma-Aldrich, USA) and 1.3 µl/ml Golgistop (BD, USA). Cells were fixed and permeabilized (eBioscience™ Foxp3/Transcription Factor Staining Buffer Set, Thermo Fisher, USA) and labelled using monoclonal antibodies (Supplemental Table 1). Cells were analysed using a LSRFortessa flow cytometer and FACSDiva software (BD, USA). Data analysis was performed with FlowJo (LLC, USA).

For FlowSOM analysis cells were manually gated (live single cells) on T cells (CD3+) and monocytic cells (CD3- CD4+) and exported for the respective analysis. This resulted in 1.1 - 6.2 $x10^5$ monocytic cells per sample and 1.4 - 6.6 $x10^5$ T cells per sample for further analysis. Markers used for FlowSOM analysis of the respective panel are shown in the heatmap (Figure 5c and 6b). Data were clustered onto a 10 node × 10 node square SOM as implemented in the CATALYST package v.1.14.1 (wrapper for FlowSOM). Lower resolution ConsensusClusterPlus metaclustering was then performed to reduce them to 8 metaclusters. Phenotypic relationship between individual clusters were explored using the UMAP algorithm

for dimension reduction of 10^5 gated cells from all samples acquired, as implemented in the runDR, runUMAP functions from the CATALYST package (R version 4.0.3). Resource intensive computation has been performed on the HPC for Research cluster of the Berlin Institute of Health.

References to the Supplementary Material

1 Schwartz, G. J. *et al.* New equations to estimate GFR in children with CKD. *J Am Soc Nephrol* **20**, 629-637, doi:10.1681/ASN.2008030287 (2009).

2 Rosario, A. S., Kurth, B. M., Stolzenberg, H., Ellert, U. & Neuhauser, H. Body mass index percentiles for children and adolescents in Germany based on a nationally representative sample (KiGGS 2003-2006). *Eur J Clin Nutr* **64**, 341-349, doi:10.1038/ejcn.2010.8 (2010).

3 Lurbe, E. *et al.* 2016 European Society of Hypertension guidelines for the management of high blood pressure in children and adolescents. *J Hypertens* **34**, 1887-1920, doi:10.1097/HJH.0000000000001039 (2016).

4 Klindworth, A. *et al.* Evaluation of general 16S ribosomal RNA gene PCR primers for classical and next-generation sequencing-based diversity studies. *Nucleic Acids Res* **41**, e1, doi:10.1093/nar/gks808 (2013).

5 Hildebrand, F., Tadeo, R., Voigt, A. Y., Bork, P. & Raes, J. LotuS: an efficient and user-friendly OTU processing pipeline. *Microbiome* **2**, 30, doi:10.1186/2049-2618-2-30 (2014).

6 Saary, P., Forslund, K., Bork, P. & Hildebrand, F. RTK: efficient rarefaction analysis of large datasets. *Bioinformatics* **33**, 2594-2595, doi:10.1093/bioinformatics/btx206 (2017).

7 Kirwan, J. A., Broadhurst, D. I., Davidson, R. L. & Viant, M. R. Characterising and correcting batch variation in an automated direct infusion mass spectrometry (DIMS) metabolomics workflow. *Anal Bioanal Chem* **405**, 5147-5157, doi:10.1007/s00216-013-6856-7 (2013).

8 Klavus, A. *et al.* "notame": Workflow for Non-Targeted LC-MS Metabolic Profiling. *Metabolites* **10**, doi:10.3390/metabo10040135 (2020).

9 Wang, Z. *et al.* Measurement of trimethylamine-N-oxide by stable isotope dilution liquid chromatography tandem mass spectrometry. *Anal Biochem* **455**, 35-40, doi:10.1016/j.ab.2014.03.016 (2014).

10 Haug, K. *et al.* MetaboLights: a resource evolving in response to the needs of its scientific community. *Nucleic Acids Res* **48**, D440-D444, doi:10.1093/nar/gkz1019 (2020).